Ettringite Formation in Heat-Cured Mortars and its Relationship to Expansion

Y. Shimada[1], P. Tennis[2], V. C. Johansen[3]
[1]Northwestern University, IL, USA; [2]Portland Cement Association, Skokie, IL, USA 60077; [3]Construction Technology Laboratory, Skokie, IL, USA 60077

1 Introduction

Delayed ettringite formation (DEF) is a form of internal sulfate attack sometimes observed in precast field concrete that has undergone high-temperature curing and subsequent exposure to moist conditions. Despite many attempts to develop fundamental understanding, the DEF mechanism is still unclear and remains controversial. In order to provide a better understanding of the DEF phenomenon, the present study [1] investigated mortar systems made with various mixing and curing parameters for detailed changes in pore solution chemistry and solid phase development, while corresponding changes in physical properties were also closely monitored. This approach enabled the development of a correlation between the chemical and physical changes and provided the opportunity for a holistic analysis. The hypothesis presented here elucidates the relationship between expansive behavior and the physical properties based on the previous paste expansion hypothesis [2], while considering observed changes in chemistry.

2 Experimental

Table 1 shows characteristics of five cements studied. Ottawa siliceous sand specified in ASTM C 778 (ASTM sand) was used to produce standard mortars. The mortar reference sand specified in EN 196-1 (EN sand) was also used for selected mixes. EN sand has a significantly wider particle size distribution than that of ASTM sand. Both sands were also tested for alkali silica reactivity following ASTM C 1260 and confirmed to be inert. Standard mortars were made with water to cement ratio of 0.485, and a lower ratio of 0.4 was used for selected mixes.

The mortar specimens were precured until initial setting at ambient temperature in 100% R.H. atmosphere. Heating and cooling rates were maintained constant at 20°C/hour. The mortar specimens were heat-cured for 12 hours at different temperatures between 23°C and 90°C in a nearly saturated atmosphere. Chamber temperature and specimen temperature were monitored for the entire curing cycle. Effects of different precuring times, heat-curing times, and heat-curing temperatures were studied.

Following the heat-curing, the mortar specimens were cooled to room temperature and stored under saturated limewater for long-term observation at ambient conditions. The specimens were kept fully immersed in the limewater where the volume ratio of solution to mortar was maintained constant at one. Each set of specimens was stored separately to prevent cross-contamination of storage solutions.

Table 1 Cement characteristics

Oxides, wt.%	C01	C03	C09	C09-III	C40
SiO_2	20.56	20.21	19.16	19.59	19.27
Al_2O_3	5.49	4.80	5.58	5.52	4.59
Fe_2O_3	2.96	3.35	2.48	2.47	2.67
CaO	61.74	65.00	63.13	62.94	62.35
MgO	2.87	1.28	2.13	2.11	3.81
SO_3	3.20	2.66	4.23	3.96	4.08
Na_2O	0.31	0.10	0.29	0.27	0.19
K_2O	0.77	0.28	0.95	0.85	1.12
N_2O eq.	0.81	0.28	0.91	0.83	0.93
Free CaO	1.00	1.07	0.34	0.31	0.81
C_3S	45	66	58	55	61
C_2S	25	8	11	14	9
C_3A	10	7	11	10	8
C_4AF	9	1	8	8	8
SSA m^2/kg	380	366	332	479	284
TOS, min.	224	240	228	190	287

The present study employed a variety of characterization techniques to evaluate physical properties of mortar systems. Expansive behavior of the mortar specimens was monitored by length change measurements. Mechanical strength was determined from resonance frequency and compressive strength tests. Electrical conductivity measurements evaluate transport property of the system and provided a measure of diffusivity. Weight changes of the specimens reflect not only cement hydration behavior but also contributions from other weight gain mechanisms. Microstructural observations provided qualitative and semi-quantitative information of pore structure of the mortar systems.

In order to keep track of chemical changes of the mortars, solid phases and pore solutions were frequently analyzed. The main interests were development of sulphoaluminate phases, especially ettringite and monosulfate, and corresponding changes in pore solution chemistry. Identification of various phases formed in the system was possible by X-ray diffraction (XRD) analysis, while ^{27}Al Magic angle spinning nuclear magnetic resonance (^{27}Al MAS NMR) was used to semi-quantitatively examine the aluminum-bearing phases. The pore solutions were analyzed for major constituents to evaluate the ion activity product (IAP) of various phases.

3 Proposed Mechanism of DEF-Related Expansion

In the course of normal cement hydration at ambient temperature, C_3A in unhydrated clinker reacts with gypsum to form ettringite, which begins immediately after mixing at ambient temperature. Initial formation of ettringite is not accompanied by expansion, as it occurs while the mixture is still plastic. This ettringite is referred as to “primary ettringite” and relatively uniformly distributed in cement paste. Alkalies in clinker phases quickly dissolve into the pore solution, while alite (and later belite) hydration forms C-S-H and calcium hydroxide. Gypsum in the system is typically depleted within a few hours of hydration. When hydration progresses at room temperature, further C_3A hydration promotes ettringite conversion into monosulfate due to sulfate deficiency in the pore solution.

When mortar specimens are subjected to a heat-curing cycle after precuring at ambient conditions, cement hydration is accelerated by increased temperature, consuming pore water at a faster rate. This leads to an increase in alkali concentration in the pore solution. Figure 1 shows changes in pore solution composition of a 90°C-cured mortar during heat-curing. Potassium and sodium concentration progressively increase as chamber temperature rises to 90°C. Until the temperature reaches 70°C, the increase in alkali species is balanced by hydroxide concentration to maintain electrical neutrality of the pore solution. Meanwhile sulfate is consumed in ongoing C_3A hydration as chamber temperature beginning to increase, and the pore solution becomes undersaturated with respect to gypsum as shown in Figure 2.

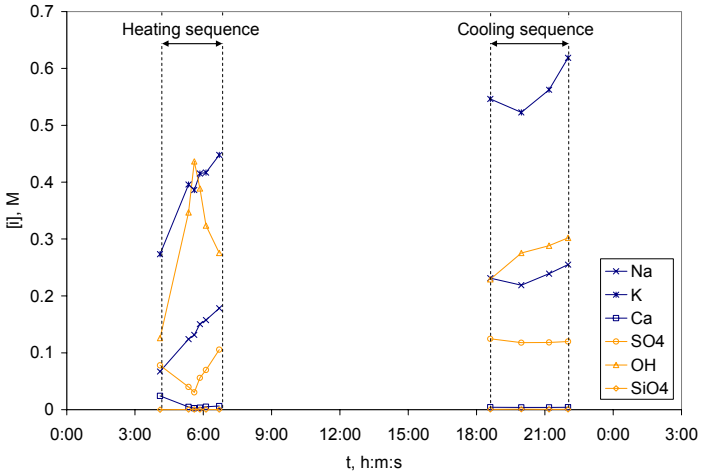

Figure 1 Changes in pore solution composition of 90°C-cured C09-III standard mortar during curing cycle. The solution was analyzed as chamber temperature reached 23, 40, 65, 70, 75, 80, and 90°C during heating sequence. After holding at 90°C for 12 hours, solution was analyzed at 90, 65, 40, and 23°C during the cooling sequence.

Ettringite becomes unstable with respect to monosulfate at higher temperature [3]. As the chamber temperature exceeds 65°C, when

corresponding specimen temperature is 55~60°C, the primary ettringite begins to partially decompose. This yields monosulfate in situ and releases excess sulfate into the pore solution, accompanied by a drop in hydroxide concentrations (Figure 1). The pore solution becomes supersaturated with respect to gypsum due to the sulfate released by the decomposition of primary ettringite (Figure 2). Famy [2] demonstrated that such sulfate is readily absorbed to C-S-H phase, which can be released when saturation ceases.

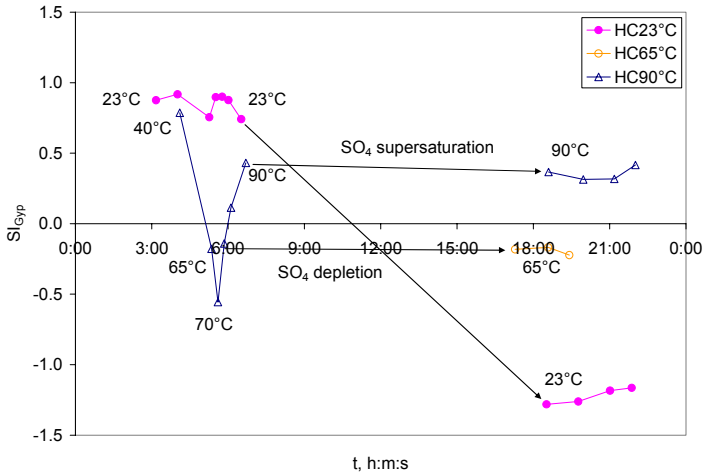

Figure 2 Changes in gypsum saturation index (SI) of C09-III standard mortars cured at various temperatures during curing cycle: $SI_{gyp} = \log(IAP_{gyp}/K_{sp})$ where SI = 0 indicates saturation, SI > 0 indicates supersaturation, and SI < 0 indicates undersaturation. The log K_{sp} values is –4.58. $IAP_{gyp} = (Ca^{2+})(SO_4^{2-})$ characterizes the stability of solid phases, i.e., the higher the IAP the more soluble the given phase. Pore solution was analyzed as chamber temperature reached 23, 40, 65, 70, 75, 80, and 90°C during heating sequence. For the cooling sequence, analysis was carried out at the holding temperature, (65°C) 40°C, and 23°C. For controls cured at 23°C, solutions were taken at the times equivalent to times when the chamber temperatures mentioned above for 90°C curing regimen were reached.

Figure 3 shows changes in ^{27}Al NMR spectra during the heat-curing, where peaks at 12.3 ppm and 9.3 ppm are assigned to aluminum in octahedral sites (Al[6]) of ettringite (AFt) and that of AFm structures, respectively [3]. In any cement system, the increase in specimen temperature results in a shift of Al[6] peak at 12.1~13.2 ppm to 9.2~9.8 ppm. This indicates thermal decomposition of primary ettringite and corresponding AFm formation. Meanwhile, alite hydration continues and a fraction of aluminum is incorporated into the C-S-H structure. Such aluminum occurs in bridging tetrahedral sites and in octahedral sites (Al[4]) of the interlayer of the C-S-H structure. In Figure 3 the Al[4] and Al[6] in C-S-H appear as a broad peak centered at about 70 ppm and a narrow peak at 5 ppm, respectively.

The ettringite (AFt) quantity relative to AFm phase was semi-quantitatively analyzed by taking the area ratio of corresponding Al[6] peaks. Figure 4

shows the rate of ettringite decomposition to AFm phase during the heating sequence, where A_t is the area under the Al[6] peak of ettringite and A_m is the area under the Al[6] peak of AFm phase. The observation suggests that the rate and extent of primary ettringite decomposition and associated monosulfate formation depend on cement characteristics. For mortars made with C01 and C09-III, primary ettringite begins disappear as chamber temperature (T_n) increases to 65°C and is completely converted to monosulfate at 90°C. On the other hand, primary ettringite remains stable until the temperature reaches 80°C for mortars made with C03 and only 59% decomposed into monosulfate at 90°C.

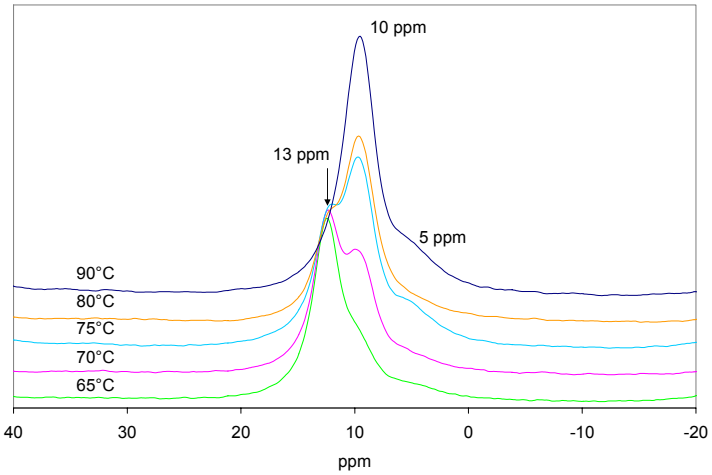

Figure 3 Changes in ^{27}Al MAS NMR spectra of C09-III standard mortars during heating sequence from 65°C up to 90°C.

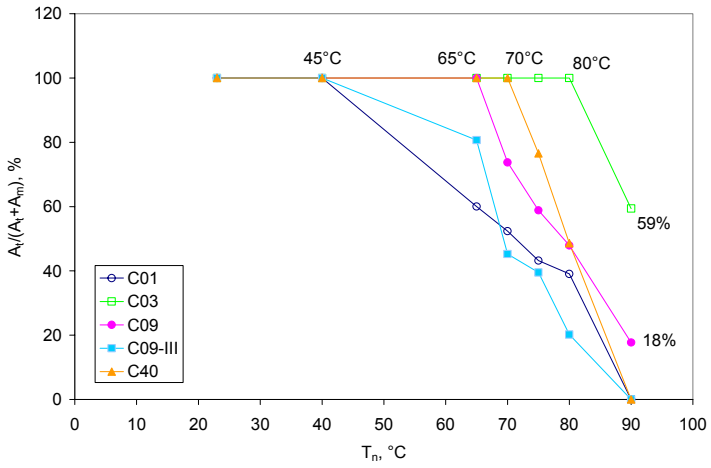

Figure 4 Changes in AFt quantity relative to AFm of standard mortars during heating sequence up to 90°C.

During the 12-hour heat curing at a designed temperature, the thermal decomposition of primary ettringite to monosulfate occurs at different rates (Figure 5). The rate of hydration and the consumption of pore water

increase with curing temperature, resulting in differences in alkali concentration between the mortars cured at different temperatures (Figure 1). The sulfate concentration clearly shows variation with the curing temperature following the heat curing, i.e., a higher curing temperature results in a higher sulfate concentration (Figure 6). The sulfate concentration in the pore solution just prior to the cooling sequence reflects the variation in the amount of sulfate taken up by the C-S-H.

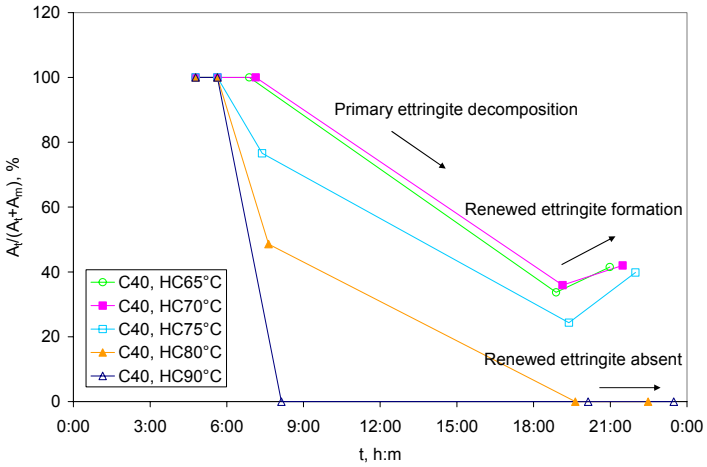

Figure 5 Changes in AFt quantity relative to AFm of C40 standard mortars during curing cycle at various temperatures.

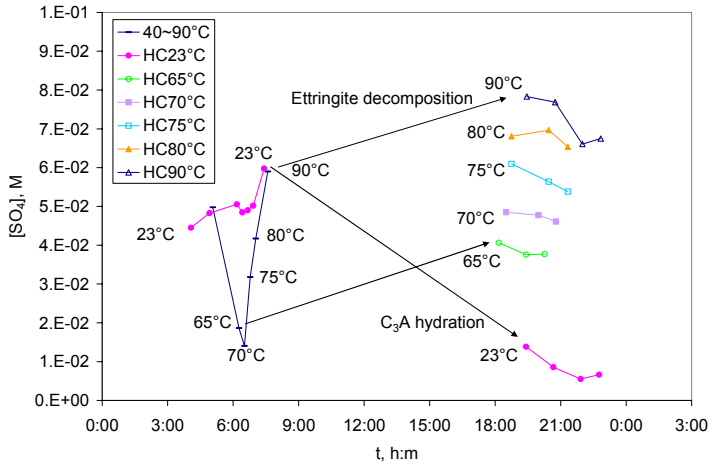

Figure 6 Changes in sulfate concentration of C01 mortars during curing cycle. The temperatures indicate chamber temperature at each data point. In order to follow the changes of 65°C-cured mortar, for example, the first data point for the control mortar provides the value at 23°C prior to the curing cycle. The first and second data points of the heating sequence to 90°C provide the value at 40 and 65°C. The 65°C curing cycle undergoes prolonged heating after this point. Three data points from the cooling sequence provides each data at 65, 40, and 23°C as chamber temperature returns to the ambient temperature.

As the system returns to ambient temperature, monosulfate becomes metastable and tends to convert back to renewed ettringite, consuming available sulfate in pore solution. Figure 5 shows recovery in ettringite content in mortars cured at 65~75°C by the end of cooling sequence, while renewed ettringite does not form during this period when cured at 80-90°C. This may suggest that increased curing temperature may delay the renewed ettringite formation. The renewed ettringite formation creates a sulfate concentration gradient between the pore solution and the C-S-H. Sulfate taken up by the C-S-H is released back into pore solution and consumed in further renewed ettringite formation.

Following a 24-hour heat-curing cycle, the mortars were submerged in saturated limewater for long-term observations. The chemical changes in the mortar systems are dominated by leaching of alkalies from the mortar matrix to the storage solution. For 90°C-cured mortars immersed in storage solution, alkali leaching occurs relatively quickly and solution exchange and alkali leaching is completed in about 84 days. This implies that the most drastic change in chemistry occurs during the first three months when cured at 90°C. The solution exchange takes longer for mortars cured at lower temperatures, e.g., 336 days for 23°C cured control mortars (Figure 7). The effect of alkali leaching on DEF-related expansion is believed to be important [2]. The stability of ettringite is controlled by the pH of the system as well as the temperature. A loss in alkalinity of the pore solution decreases the solubility of ettringite, which facilitates renewed ettringite formation. Sulfate consumption by the ettringite creates a sulfate concentration gradient between the pore solution and C-S-H, and the sulfate release persists as it is continuously consumed by further renewed ettringite formation.

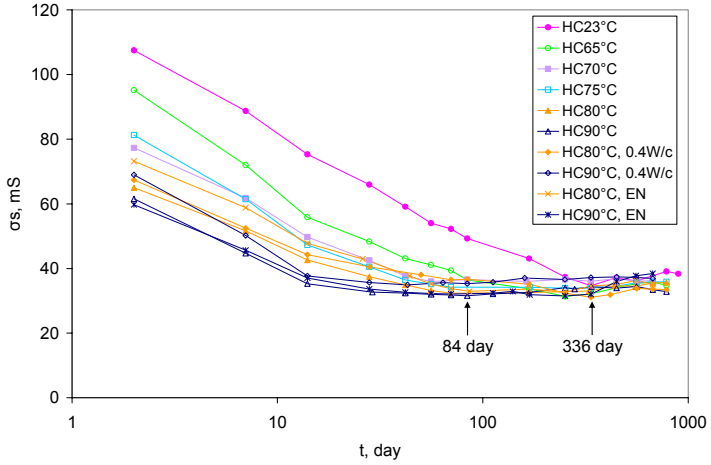

Figure 7 Changes in pore solution conductivity of C09 mortars during storage under saturated limewater.

Renewed ettringite formation begins within days of storage under limewater for the 90°C-cured mortar, and the saturation of pore solution with respect to gypsum persists only for a week. The majority of renewed ettringite relative to AFm phase forms in the system prior to the onset of expansion (Figure 8). The subsequent expansion is attributed to relatively minor remainder of ettringite yet to nucleate. Once mortar structure is weakened by various structural defects, large expansion could be produced by relatively small stress.

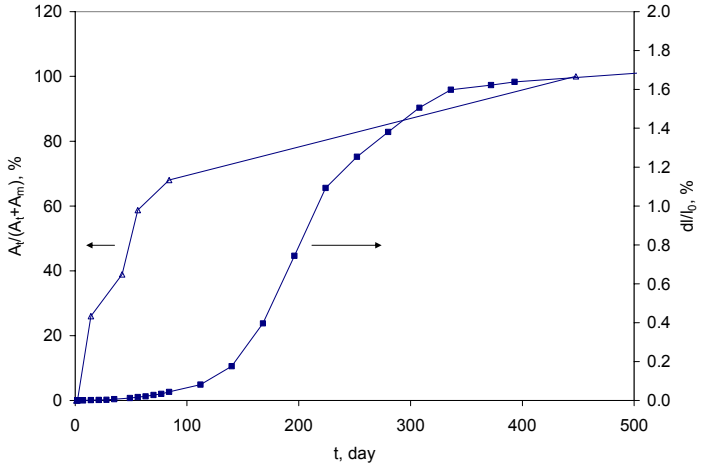

Figure 8 Changes in AFt quantity relative to AFm and expansive behavior of 90°C-cured C40 standard mortar.

The paste expansion hypothesis [2, 5] attributes the cause of expansion to the renewed ettringite formed in situ within nanoscale mesopores distributed throughout the paste (Figure 9). The nucleation and growth of renewed ettringite in situ, directly on the monosulfate in mesopores, within already hardened cement paste as nanoscale crystals is accompanied by expansive stress. However, such deleterious renewed ettringite (DRE) crystals are unstable with respect to larger crystals. In order to minimize surface energy, very fine DRE crystals dissolve into pore solution and recrystallize as innocuous renewed ettringite (IRE) in the largest spaces available. This is a classic aging process, known as Ostwald ripening, which occurs in any cementitious material regardless of their curing history. Ettringite depositions often observed in pores and cracks of DEF-affected materials by SEM examination are the consequence of visible IRE formation.

The formation and growth of IRE is not the cause of expansion. When the nanoscale DRE forming within the cement paste dissolves and recrystallizes in the open spaces, the expansive pressure exerted on the pore walls is relieved. In other words, Oswald ripening process acts as a stress relief mechanism in DEF phenomena. The growth of fine DRE crystals within the paste causing expansion and Oswald ripening process

promoting the dissolution of such DRE take place simultaneously. Therefore, there exist two competing mechanisms in the occurrence of DEF-related expansion. When the dissolution of DRE by Ostwald ripening is slower than its growth in a mesopore, the ettringite crystals may exert expansive pressure on the pore wall.

The paste expansion hypothesis is in accordance with changes observed in normalized conductivity of expansive mortars. The normalized conductivity provides a measure of the diffusivity, that is, the higher the normalized conductivity, the easier the ionic transport through the system is. Figure 10 shows a small increase in the normalized conductivity at the very early period of storage, while the mortar exhibits little expansion. This is followed by another abrupt increase in the normalized conductivity, which is concurrent with the onset of expansion as determined from the first inflection point of the expansion curve. This observation indicates that nucleation of DRE in mesopores leads to an increase in capillary porosity, which resulted in a relatively small increase in diffusivity immediately after the curing cycle. The DRE formation causes a volume increase of the paste and gives rise to local strain and introduces various structural defects due to variation in local conditions, e.g., varying density of paste and differences in the rate of expansion. This defect formation weakens the structure and decreases resistance to further expansive pressure within the paste. While structural defects develop throughout the paste, the capillary porosity continues to increase with ongoing paste expansion. This enhances pore connectivity and drastically increases overall diffusivity. This is corroborated by weight gain behavior of the system, which is caused by cement hydration, ettringite formation, and structural defects filled with water. Observed changes in the diffusivity shows reasonable agreement with the model developed upon assumption that the diffusivity of the system increases with the degree of expansion due to introduction and extension of structural defects.

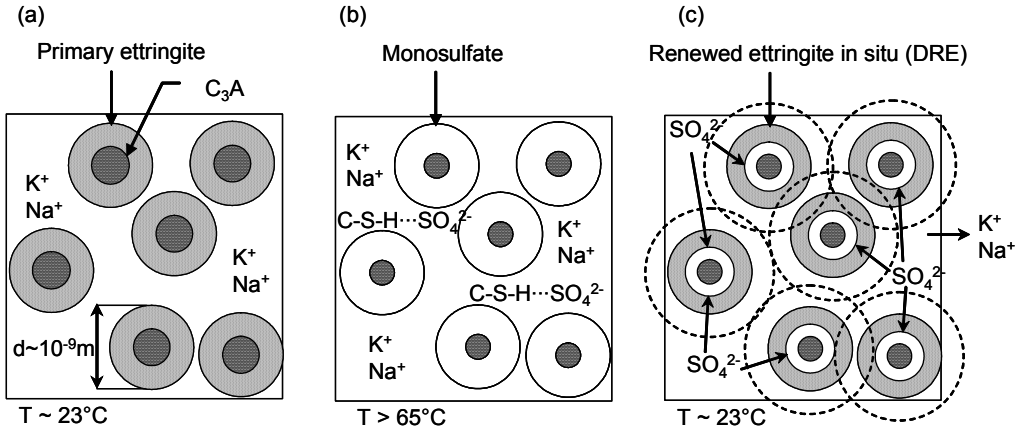

Figure 9 Schematic representation of paste expansion hypothesis: (a) The normal C_3A hydration with gypsum forming primary ettringite at ambient temperature, (b) thermal

decomposition of the primary ettringite and monosulfate formation, releasing excess sulfate that are adsorbed to C-S-H, and (c) renewed ettringite formation in situ associated with a decrease in temperature and alkalinity of the system with a supply of sulfate from the C-S-H, which is accompanied by expansive pressure. Dashed line indicates volume influenced by the expansive pressure.

The onset of expansion appears to roughly coincide with the onset of defect formation determined by different physical testing. Normalized conductivity measurements find that the defect formation is preceded by paste expansion up to about 0.05%. The change in resonance frequency and compressive strength, providing measures of mechanical strength, also shows significant loss of strength at about 0.1~0.2% of expansion. This is also suggested by Scherer (2002) who noted that cementitious materials could tolerate strains of approximately 0.05% with a reasonable rate of creep.

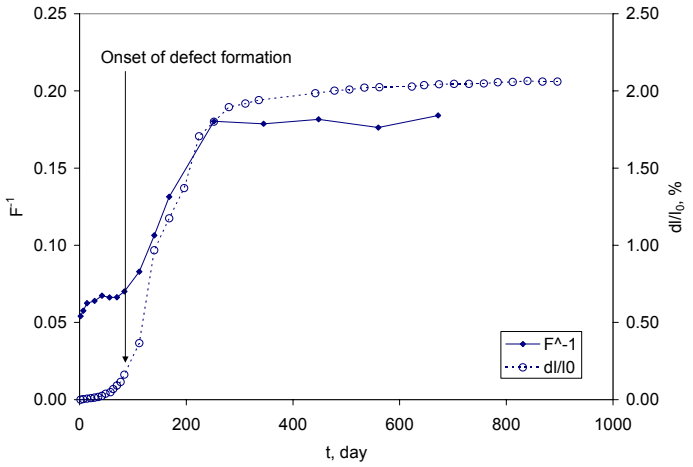

Figure 10 Interpretation of changes in normalized conductivity measured (F^{-1}), model (F^{-1}), and model for cement paste (F_p^{-1}) of 90°C-cured C40 mortar and its expansive behavior.

Various physical testing employed here provide quantitative importation on microstructural characteristics of mortar systems. In general, the mortars characterized with high mechanical strength and low diffusivity have microstructures relatively dense and tightly compacted, where the ionic transport is rather slow. In contrast, the mortars characterized with low strength and high diffusivity have coarse microstructures possibly containing inherent flaws in the microstructure, providing high connectivity between pores and other defects. Table 2 shows that a reduced w/c ratio of mortar made with C09 from 0.485 to 0.4 results in an increase in resonance frequency (F) and a reduced normalized conductivity (F^{-1}). This is a reflection of decreased capillary porosity and increased paste density, indicating altered microstructure. Similarly, using finer EN sand instead of ASTM sand with C09 cement gave rise to a better particle packing and a denser microstructure, which led to an increase in strength accompanied

by a reduced diffusivity. This is also observed with C09-III cement. An important observation in this study is that the greater the mechanical strength and the lower the diffusivity of the system, the higher is the final expansion. In other words, the expansion is more severe in the system with a dense microstructure.

Table 2 Mixing parameters of mortars cured at 90°C for 12 hours following precuring for TOS and relationship between physical properties of the mortar, namely resonance frequency at 7 day (F) and normalized conductivity at 2 day (F^{-1}), and the degree of expansion.

Cement	Sand	W/c	dl/l_0 final, %	F, Hz	F^{-1}
C09	ASTM	0.485	0.8238	1152	8.47E-02
C09	ASTM	0.400	0.9268	1185	5.24E-02
C09	EN	0.485	1.1684	1185	7.00E-02
C09-III	ASTM	0.485	0.2090	1139	7.34E-02
C09-III	EN	0.485	1.3234	1178	6.81E-02

The competition between the two processes is largely influenced by the microstructural characteristics of the system (Figure 11). In a well-connected, porous microstructure containing many flaws or structural defects, DRE easily finds the paths to larger spaces, which promotes dissolution of the fine DRE crystals within the paste. Thus, the stress relief mechanism would be facilitated. On the other hand, in a well-compacted tight microstructure with fewer pores, the fine DRE would stay in the paste for a much longer time and maintain the expansive pressure, resulting in a more severe expansion. This accounts for the observed relationship between the physical characteristics and expansive behavior. Thus, DEF-prone system can be characterized by high mechanical strength and low diffusivity, whereas DEF-resistant system can be characterized by low mechanical strength and high diffusivity.

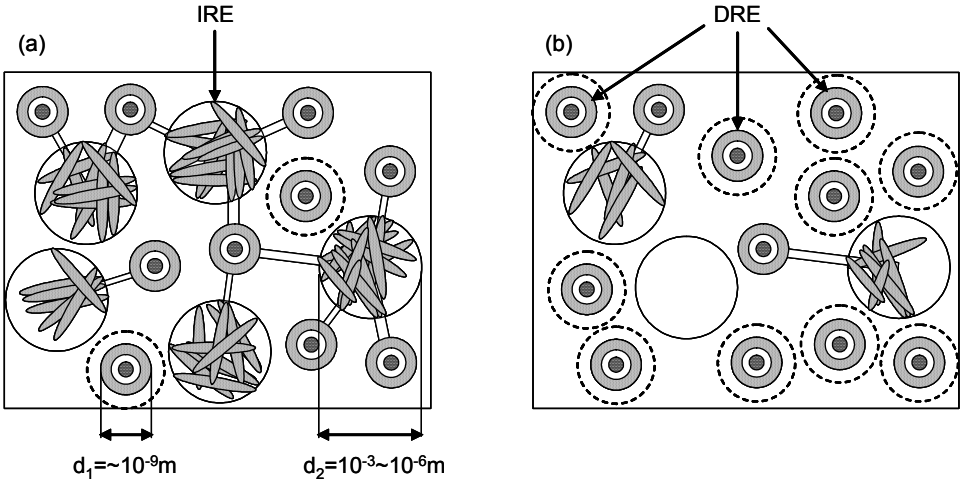

Figure 11 Schematic representation of (a) a well-connected porous microstructure with many flaws where the Ostwald ripening process is facilitated leading to a relaxation of expansive pressure, and (b) a well-compacted tight microstructure with fewer pores

where Ostwald ripening process is impeded leading to a development of expansive pressure. Dashed line indicates volume influenced by the expansive pressure.

After major changes in pore solution chemistry associated with solution exchange ceases, Ostwald ripening governs the kinetics. Ostwald ripening is a slower process compared to alkali leaching. The chemical potential gradient between crystals in a mesopore and a micropore is much smaller than the gradient between the pore solution and storage solution. Thus, the rate of renewed ettringite formation slows down significantly after the first 84 days for 90°C-cured mortars.

4. Conclusions

A holistic approach reveals relationships between the physical properties and expansive behavior of mortar systems. High-temperature curing of portland cement systems results in formation of fine ettringite crystals widely distributed within the hardened cement paste. Subsequent growth of those crystals leads to possible expansive pressure. Concurrently, the normal aging process of mortar systems involves dissolution of fine ettringite and subsequent recrystallization as innocuous crystals in the largest accessible spaces. Ostwald ripening processes facilitate relaxation of any expansive pressure developed within the paste. These competing physiochemical phenomena dictate the expansive stress developed. The rate of Ostwald ripening is rather slow in well-compacted, dense microstructures containing few flaws. Altering the mortar characteristics to increase the diffusion rate decreases the risk of DEF-related expansion and vice versa. Having information on microstructural characteristics, or physical properties, of the system is essential in order to fully understand DEF-related expansion. Considering both physical and chemical characteristics together may drastically improve the quality of DEF risk management.

5. References

[1] Shimada, Y., *Chemical Path of Ettringite Formation in Heat-Cured Mortar and Its Relationship to Expansion,* SN2526, Portland Cement Association, Skokie, Illinois, USA, 2005, 507 pages.

[2] Famy, C., *Expansion of Heat-Cured Mortars*, Thesis (Ph.D.), University of London, 1999, 304 pages.

[3] Shimada, Y. and Young, J. F., “Thermal Stability of Ettringite in Alkaline Solution at 80°C,” *Cement and Concrete Research*, Vol. 34, 2004, pages 2261 to 2268.

[4] Scherer, G.W., “Factors Affecting Crystallization Pressure,” *Proceedings of the International RILEM TC 186-ISA Workshop on Internal Sulfate Attack and Delayed Ettringite Formation*, Villars, Switzerland, September 2002, pages 139-154.

[5] Famy, C., Scrivener, K.L., Brough, A. D., "Role of Microstructural Characterization in Understanding the Mechanism of Expansion Due to Delayed Ettringite Formation," *Proceedings of the International RILEM TC 186-ISA Workshop on Internal Sulfate Attack and Delayed Ettringite Formation*, Villars, Switzerland, September 2002, pages 167-172.